

Transport Properties and Density of States of Quantum Wires with Off-diagonal Disorder

P. W. Brouwer^{ab*}, Christopher Mudry^{ac†} and Akira Furusaki^{d‡}

^aLyman Laboratory of Physics, Harvard University, Cambridge, MA 02138, USA

^bLaboratory of Atomic and Solid State Physics, Cornell University, Ithaca, NY 14853, USA

^cPaul Scherrer Institut, CH-5232, Villigen PSI, Switzerland

^dYukawa Institute for Theoretical Physics, Kyoto University, Kyoto 606-8502, Japan

Abstract

We review recent work on the random hopping problem in a quasi-one-dimensional geometry of N coupled chains (quantum wire with off-diagonal disorder). Both density of states and conductance show a remarkable dependence on the parity of N . The theory is compared to numerical simulations.

PACS: 71.55.Jv, 71.23.-k, 72.15.Rn, 11.30.Rd

Keywords: Disordered Systems, Mesoscopic Systems, and Critical Phenomena.

1. Introduction and Results

With the realization that the problem of Anderson localization is amenable to a RG analysis came the understanding that some transport and spectral properties of a quantum particle subjected to a weak random potential depend qualitatively only on dimensionality and the symmetries of the random potential [1]. For essentially all types of randomness the dimensionality two of space plays the role of the lower critical dimension: Below two dimensions and for arbitrary weak disorder a quantum particle is always localized (i.e., the wavefunction is insensitive to a change in boundary conditions, or, equivalently, exponential decay of the conductance with sys-

tem size), whereas a finite amount of disorder is needed to localize a quantum particle in three dimensions.

A notorious exception to this rule is the case of a particle on a single chain with random nearest neighbor hopping which appears in many reincarnations, e.g., random XY spin chains [2] and diffusion in random environments [3]. In all these cases, the cause underlying the different behavior of random systems with off-diagonal disorder is the existence of a sublattice, or *chiral*, symmetry, which is absent for diagonal disorder [4].

The purpose of this contribution is to review our recent work (together with Simons and Altland [5]) on the random hopping problem in a quasi-one-dimensional “wire” geometry [5–8]. We consider the density of states (DoS) and conductance, and focus on the differences between the cases of off-diagonal and diagonal disorder in the localized regime. (For off-diagonal disorder, we assume absence of diagonal disorder.) The quantum wire is the logical intermediate be-

*Work at Harvard is supported by NSF grants nos. DMR 94-16910, DMR 96-30064, and DMR 97-14725.

†Supported in part by a grant from the Swiss Nationalfonds.

‡Supported in part by Grant-in-Aid for Scientific Research (No. 11740199) from the Ministry of Education, Science, Sports and Culture, Japan. The numerical calculations were performed at the Yukawa Institute Computer Facility.

tween one and two dimensions.¹ The quasi-one-dimensional geometry allows us to find exact solutions for the conductance at the band center $\varepsilon = 0$ and the DoS near $\varepsilon = 0$, while, in contrast to purely one-dimensional counterparts, it still shows a crossover from a diffusive to a localized regime, as is the case in two dimensions.

In the diffusive regime, differences between off-diagonal and diagonal disorder are limited to small quantum corrections to the DoS and conductance. The DoS near $\varepsilon = 0$ follows from the so-called ‘‘chiral’’ random matrix theory (RMT), which was originally proposed in the context of quenched approximations to the QCD Hamiltonian [11]. In chiral RMT, all eigenvalues come in pairs $\pm\varepsilon$. For N coupled random hopping chains, level repulsion between the smallest eigenvalue above the band center $\varepsilon = 0$ and its mirror image then leads to a suppression of the DoS near $\varepsilon = 0$,

$$d\mathcal{N}/d\varepsilon \propto v_F^{-1}(\varepsilon/\Delta)^{\beta-1}, \quad 0 < \varepsilon \ll \Delta. \quad (1)$$

Here $d\mathcal{N}/d\varepsilon$ is the DoS per unit volume, v_F is the Fermi velocity, $\Delta = 2\pi v_F/NL$ is the mean level spacing, and the symmetry index $\beta = 1$ in the presence of both time-reversal and spin-rotational symmetry and $\beta = 2$ (4) if time-reversal symmetry (spin-rotational symmetry) is broken. Several level spacings away from the center of the band, the mirror symmetry of the spectrum plays no important role, and the level statistics were found to agree with those of the standard RMT. Similarly, different quantum corrections to the conductance are obtained for energies close to the band center [6].

On the other hand, beyond the diffusive regime, i.e., for sample lengths $L \gtrsim \xi$, where ξ is a crossover length scale (to be defined after Eq. (4) below), quantum corrections are dominant, and the differences between diagonal and off-diagonal disorder can be much more dramatic. While for diagonal disorder, the DoS is constant as $\varepsilon \rightarrow 0$, Dyson showed that for off-diagonal disorder $d\mathcal{N}/d\varepsilon$ diverges upon approaching the band

¹Two dimensional models with off-diagonal disorder are also studied in the context of strongly interacting electron systems [9]. We refer the reader to Ref. [10] for a review of work done on the two dimensional case.

center [12] :

$$\frac{d\mathcal{N}}{d\varepsilon} \propto \frac{1}{\xi|\varepsilon \ln^3(\varepsilon\xi/v_F)|}, \quad 0 < \varepsilon\xi/v_F \ll 1. \quad (2)$$

Note that, in contrast to the diffusive regime (1), the energy scale that governs the divergence does not depend on the system size, nor does the form of the singularity depend on the symmetry index β . For N coupled chains, Dyson’s result (2), remains valid for odd N ,² but not for even N [8]: For an even number of chains, the DoS diverges only logarithmically for $\beta = 1$, whereas $d\mathcal{N}/d\varepsilon$ shows a pseudogap for $\beta = 2, 4$,

$$\frac{d\mathcal{N}}{d\varepsilon} \propto \frac{1}{v_F} \left(\frac{\varepsilon\xi}{v_F} \right)^{\beta-1} \left| \ln \frac{\varepsilon\xi}{v_F} \right|, \quad 0 < \frac{\varepsilon\xi}{v_F} \ll 1. \quad (3)$$

The relevant energy scale, however, remains the same as in Eq. (2). The even-odd effect in the DoS around $\varepsilon = 0$ is accompanied by an even-odd effect for the conductance g at the band center [5–7]. For odd N , there is no exponential localization; g has a broad distribution, with fluctuations that are of the same order as the average,

$$\langle \ln g \rangle = -4\sqrt{\frac{L}{\beta\pi\xi}}, \quad \text{var } \ln g = \frac{8(\pi-2)L}{\beta\pi\xi}, \quad (4)$$

where the crossover length scale $\xi = (\beta N + 2 - \beta)\ell/\beta$, and ℓ is the mean free path. (For small N there are corrections due to the appearance of a second dimensionless parameter needed to characterize the off-diagonal disorder, see Ref. [7] for details.) In contrast, for even N , g is exponentially small, its distribution being close to log-normal,

$$\langle \ln g \rangle = -\frac{2L}{\xi} + \sqrt{\frac{8L}{\beta\pi\xi}}, \quad \text{var } \ln g = \frac{8(\pi-1)L}{\beta\pi\xi}. \quad (5)$$

In this case, ξ can be interpreted as the localization length. Away from the band center and for diagonal disorder, $\langle \ln g \rangle = -(1/2)\text{var } \ln g = -2L/\xi'$, with $\xi' = (\beta N + 2 - \beta)\ell$, irrespective of the parity of N , as for quantum wires with diagonal disorder [13]. Note that for even N , despite the similarities, differences between off-diagonal

²The proportionality constants in Eqs. (2) and (3) may depend on N .

and diagonal disorder persist, though they are more subtle.

In the remaining sections of this paper, we review the theory describing these two parity effects.

2. Two microscopic models

2.1. Lattice model

The random hopping model is a lattice model with nearest neighbor hopping only, where the hopping amplitude takes a different (random) value between adjacent sites. In our case we consider a two-dimensional square lattice, for which the Schroedinger Equation takes the form

$$\mathcal{H}\psi_{i,j} = \sum_{\pm} (t_{i,j;i\pm 1,j}\psi_{i\pm 1,j} + t_{i,j;i,j\pm 1}\psi_{i,j\pm 1}). \quad (6)$$

Hermiticity requires $t_{i,j;i\pm 1,j} = (t_{i\pm 1,j;i,j})^*$ and $t_{i,j;i,j\pm 1} = (t_{i,j\pm 1;i,j})^*$. We consider a quasi-one-dimensional geometry (length L of the disordered region much larger than its width Na , where N is the number of chains and a the lattice constant), with open boundary conditions in the transverse direction: $t_{0,j;1,j} = t_{N,j;N+1,j} = 0$. On the left ($j < 0$) and right ($j > L/a$), the disordered region is attached to ideal leads ($t_{i,j;i\pm 1,j} = t_{\parallel}$, $t_{i,j;i,j\pm 1} = t_{\perp}$ for $j < 0$ or $j > L/a$). In the disordered region, the hopping amplitudes show fluctuations around the average values t_{\parallel} and t_{\perp} , respectively. The fluctuations are real, complex, or quaternion, for the symmetry classes $\beta = 1, 2, \text{ and } 4$, respectively.

The random flux model is a special version of the random hopping model for which each plaquette is threaded by a random flux. In that case, the hopping amplitudes have magnitude t and a random phase $\phi_{i,j;i\pm 1,j}$, so that the total phase accumulated going around a plaquette equals the phase through the plaquette in units of the flux quantum Φ_0 .

The random hopping model is special because of the existence of a sublattice symmetry: Under a transformation

$$\psi_{i,j} \rightarrow (-1)^{i+j}\psi_{i,j},$$

the Hamiltonian changes sign. Hence, if ε is an eigenvalue of \mathcal{H} , then $-\varepsilon$ is so as well. The band

center $\varepsilon = 0$ is a special energy with respect to this transformation. As we shall see below, it is the existence of this extra symmetry that causes the spectral and transport properties of the random hopping model at the band center to be so dramatically different from those of models with on-site disorder. For historical reasons, the sublattice symmetry is referred to as *chiral* symmetry.

2.2. Continuum model

While the lattice version (6) of the random hopping model is the version that is usually considered in the literature, we use a different (continuum) model for our analytical calculations,

$$\mathcal{H}_{\text{cont}}\psi(y) = [i\sigma_3\partial_y + \sigma_3v(y) + \sigma_2w(y)]\psi(y). \quad (7)$$

Here ψ is a $2N$ component vector (elements of ψ occur in pairs that correspond to left and right movers), v and w are $N \times N$ random Hermitian matrices, and the σ_{μ} ($\mu = 1, 2, 3$) are the Pauli matrices. In Eq. (7) and below we choose our units such that the Fermi velocity $v_F = 1$. The chiral symmetry is now represented by

$$\sigma_1\mathcal{H}_{\text{cont}}\sigma_1 = -\mathcal{H}_{\text{cont}}.$$

For $\beta = 1$, w (v) is (anti-)symmetric; for $\beta = 4$, w (v) is (anti-)self dual. The disorder potentials v and w are chosen independently and Gaussian distributed with zero mean and with variance

$$\langle v_{ij}(y)v_{kl}^{\dagger}(y') \rangle = \frac{\delta(y-y')}{\xi} \left(\delta_{ik}\delta_{jl} - \frac{2-\beta}{\beta}\delta_{il}\delta_{jk} \right),$$

$$\langle w_{ij}(y)w_{kl}^{\dagger}(y') \rangle = \frac{\delta(y-y')}{\xi} \left(\delta_{ik}\delta_{jl} + \frac{2-\beta}{\beta}\delta_{il}\delta_{jk} \right),$$

respectively. (For small N a slightly more general form of the variance is needed, see [7].) The justification for this change of models is our anticipation that, for weak disorder and for a sufficiently large system size, only the fundamental symmetries of the microscopic model are relevant. In order to verify this assumption of universality, we compare the theoretical predictions based on Eq. (7) below to numerical simulations of the lattice model (6).

3. Fokker-Planck approach

3.1. General method

Spectral and transport properties of the continuum model (7) can be studied in a unified way from the statistical distribution of the *reflection matrix* $r(\varepsilon)$ of the disordered wire. The reflection matrix is defined from the relation between the amplitudes $\psi_\varepsilon^{\text{iL}}$ and $\psi_\varepsilon^{\text{oL}}$ of an incoming and an outgoing wavefunction at energy ε on the same (left) side of the disordered region (Fig. 1),

$$\psi_\varepsilon^{\text{oL}} = r(\varepsilon)\psi_\varepsilon^{\text{iL}}. \quad (8)$$

Transport properties (the conductance G) follow from the eigenvalues of $r^\dagger r$, when the right side of the quantum wire is attached to a lead (Fig. 1a),

$$G = \frac{2e^2}{h} g, \quad g = \text{tr} (1 - r^\dagger r), \quad (9)$$

while the DoS is obtained from the eigenphases of r when the quantum wire is closed at the right side [14] (Fig. 1b)

$$\frac{d\mathcal{N}}{d\varepsilon} = \frac{1}{2\pi i N L} \text{tr} \left(r^\dagger \frac{\partial}{\partial \varepsilon} r \right). \quad (10)$$

The distribution of r is computed using a RG approach: One calculates how the eigenvalues of $r^\dagger r$ (in the case of the conductance) or the eigenphases of r (in the case of the DoS) change when a thin slice is added to the disordered region (Fig. 2). If we place the thin slice to the left of the disordered region, the change of the reflection matrix is given by

$$r \rightarrow r_1 + t'_1 (1 - r r'_1)^{-1} r t_1, \quad (11)$$

where r_1 and r'_1 (t_1 and t'_1) are the reflection (transmission) matrices of the thin slice (Fig. 2). If the length δL of the thin slice is much smaller than a mean free path, these can be computed using the Born approximation,

$$\begin{aligned} r_1 &= -W + \frac{1}{2}(VW - WV), \\ t_1 &= 1 + iV - \frac{1}{2}(V^2 + W^2) + i\varepsilon\delta L, \\ r'_1 &= W + \frac{1}{2}(VW - WV), \\ t'_1 &= 1 - iV - \frac{1}{2}(V^2 + W^2) + i\varepsilon\delta L, \end{aligned} \quad (12)$$

where $V = \int_0^{\delta L} dy v(y)$, and $W = \int_0^{\delta L} dy w(y)$. Here we neglected terms that are of order δL^2 . Together with the distribution of the disorder potentials w and v , Eqs. (11)–(12) define how the distribution of the reflection matrix r evolves with the length L of the quantum wire. The RG approach can be represented in terms of a Fokker-Planck equation describing the “Brownian motion” of the eigenvalues of $r^\dagger r$ or eigenphases of r in the geometry of Fig. 1a and 1b, respectively.

Equations (11)–(12) are exact for the continuum model (7). A different choice for the distribution of v and w , or use of the lattice model (6) instead of Eq. (7), would have led to different statistical properties of the scattering matrix for a thin slice. However, as we have verified numerically, such differences are irrelevant in the RG sense, i.e., they disappear for sufficiently long wires (longer than the mean free path ℓ) and weak disorder (ℓ much larger than the lattice constant a).

3.2. DoS

Since the quantum wire is closed at one end, the initial condition at $L = 0$ for the RG equation (11) is $r = 1$. The RG flow ensures that the reflection matrix r remains a $N \times N$ unitary matrix for all L . Hence, for all L there exists a Hermitean $N \times N$ matrix Φ with $r = \exp(i\Phi)$. The eigenvalues ϕ_j of Φ are the eigenphases of r . The change of Φ under the increment (11)–(12) is

$$\cot \left(\frac{\Phi}{2} \right) \rightarrow e^{-(W+iV)} \cot \left(\frac{\Phi}{2} + \varepsilon\delta L \right) e^{-(W-iV)}$$

up to second order in V and W and first order in ε . Taking the length L as a fictitious “time”, the eigenphases ϕ_j of Φ perform a Brownian motion on the unit circle, which is such that upon increasing L , they move (on average) counterclockwise. Integration of Eq. (10) yields a relation between the ϕ_j and the DoS valid in the limit of large L ,

$$\mathcal{N}(\varepsilon') = \int_0^{\varepsilon'} d\varepsilon \frac{d\mathcal{N}}{d\varepsilon} = \frac{1}{2\pi N} \sum_j \frac{\partial \phi_j}{\partial L}. \quad (13)$$

[Note that for $\varepsilon = 0$, $\phi_j = 0$ for all L .] Hence, to find the (average) DoS per unit volume, we compute the (average) “current” of the eigenphases

ϕ_j moving around the unit circle and differentiate to energy. We remark that, in the absence of disorder, the angles ϕ_j move around at a constant speed $\propto \varepsilon$, resulting in a constant DoS. With disorder, their motion acquires a random (Brownian) component, which dramatically affects their average speed, and hence the DoS.

For a quantitative description a different parameterization of the eigenphases of the reflection matrix is more convenient,

$$\tan(\phi_j/2) = \exp(u_j), \quad (14)$$

where the u_j are restricted to the two branches $\text{Im } u_j = 0$ and $\text{Im } u_j = \pi$ in the complex plane (Fig. 3). Starting from the RG equation (11), one then obtains that the joint probability distribution $P(u_1, \dots, u_N)$ for the u_j obeys

$$\begin{aligned} \frac{\partial P}{\partial L} &= \sum_j \frac{\partial}{\partial u_j} \left[\frac{4}{\beta\xi} J \frac{\partial}{\partial u_j} J^{-1} - 2\varepsilon \cosh(u_j) \right] P, \\ J &= \prod_{j < k} \sinh^\beta[(u_j - u_k)/2]. \end{aligned} \quad (15)$$

This Fokker-Planck equation describes the motion of N fictitious Brownian “particles” with coordinates u_j ($j = 1, \dots, N$) and diffusion coefficient $4/\beta\xi$, subject to a driving force $F_\varepsilon = 2\varepsilon \cosh u_j$ and a *long-range* repulsive two-body interaction $F_{\text{int}} = (2/\xi) \coth[(u_j - u_k)/2]$. The parameterization (14) is such that a Brownian particle with coordinate u_j that vanishes on one of the branches at $\pm\infty$ reappears at the opposite branch (dotted arrows in Fig. 3).

Analysis of the Brownian motion described by Eq. (15) then leads to the asymptotes (2,3) for the DoS in the random hopping model. A detailed derivation of these results based on an estimate of the steady-state-current supported by Eq. (15) can be found in Ref. [8]. Here we present only a brief sketch, focusing on the origin of the even-odd effect: The competition between the driving force F_ε and diffusion on the one side, and the long-range repulsive two-body interaction F_{int} on the other side. The driving force F_ε pushes the particles to the right (left) on the lower (upper) branch and thus causes the nonzero steady-state-current. Diffusion keeps the particles mobile where the driving force F_ε is small,

thus enhancing the current, and hence the DoS [8]. The long-range repulsion F_{int} , on the other hand, traps an equal number of the particles in two “traps” near $u = \ln(\varepsilon\xi)$ and $u = -\ln(\varepsilon\xi) + \pi i$, and thus tends to suppress the DoS. For even N , all particles are trapped ($N/2$ particles in each trap). Rare events caused by particles that are “thermally” excited out of their traps still allows for a small “current”, resulting in the small DoS in Eq. (3) (Fig. 3a). For odd N , however, only $(N - 1)/2$ particles are trapped near each end point, while one particle is left alone, unaffected by the long-range repulsion (Fig. 3b). Motion of this particle is dominated by diffusion, which explains the enhancement of the DoS for odd N .

The agreement between the theory and numerical simulation of the lattice random hopping model is excellent as is depicted in Fig. 4.

3.3. Conductance

The chiral symmetry results in the symmetry relation $r(\varepsilon) = r(-\varepsilon)^\dagger$ [6]. Hence, at the band center, the reflection matrix is Hermitean. We parameterize the eigenvalues of r as $\tanh x_j$, where the x_j are N real numbers, and formulate the RG approach of Sec. 3.1 as a Brownian motion process for the x_j . Away from the band center, only the eigenvalues $\tanh^2 x_j$ of the product $r^\dagger r$ can be studied in the RG approach: In this case, the sign of the x_j has no relevance, since $r^\dagger r$ does not change under $x_j \rightarrow -x_j$.

In terms of the x_j , the conductance reads

$$g = \sum_j (1 - \tanh^2 x_j) = \sum_j \cosh^{-2} x_j. \quad (16)$$

The RG equation (11) then leads to a Fokker-Planck equation for the L -evolution of the joint probability distribution $P(x_1, \dots, x_N)$ at the band center [5–7],

$$\begin{aligned} \frac{\partial P}{\partial L} &= \frac{1}{\beta\xi} \sum_{j=1}^N \frac{\partial}{\partial x_j} \left[J \frac{\partial}{\partial x_j} (J^{-1} P) \right], \\ J &= \prod_{k > j} |\sinh(x_j - x_k)|^\beta. \end{aligned} \quad (17)$$

Sufficiently far away from the band center, the L -evolution of the x_j 's is the same as for a quantum

wire with on-site disorder, which is given by the well-known DMPK equation [15]

$$\frac{\partial P}{\partial L} = \frac{1}{2\xi'} \sum_{j=1}^N \frac{\partial}{\partial x_j} \left[J \frac{\partial}{\partial x_j} (J^{-1}P) \right], \quad (18)$$

$$J = \prod_{k>j} |\sinh^2 x_j - \sinh^2 x_k|^\beta \prod_k |\sinh(2x_j)|,$$

where $\xi' = (\beta N + 2 - \beta)\ell$.

Both Fokker-Planck equations describe the Brownian motion of N particles with the coordinate x_j on the real axis and interacting through a hardcore repulsive two-body potential (Fig. 5). Far away from the band center, a particle at position x_j is also repelled by the mirror image at position $-x_j$ as is required by the symmetry of $r^\dagger r$ under $x_j \rightarrow -x_j$. For each x_j , the repulsion from the mirror image $-x_j$ ensures that all x_j increase linearly with L , thus causing the exponential decay of g with L . On the other hand, at the band center the sign of x_j matters since there is no repulsion from mirror images. For odd N there will be no net force on the particle with coordinate $x_{(N+1)/2}$ (for large L). Hence $x_{(N+1)/2}$ remains close to the origin, while all other x_j increase (or decrease) linearly with L . The coordinate $x_{(N+1)/2}$ dominates the conductance, its fluctuations leading to the $(L/\xi)^{1/2}$ dependence of $\ln g$ in Eq. (4). For even N no such “exceptional” particle exists; all x_j increase (if they are positive) or decrease (if they are negative) linearly with L , causing the conductance to be exponentially small, cf. Eq. (5).

We refer the reader to Refs. [6] for the detailed calculation of the moments of the conductance. The agreement between the theory and numerical simulations of the random flux case is excellent as is illustrated in Fig. 6.

REFERENCES

1. For a review, see P. A. Lee and T. V. Ramakrishnan, *Rev. Mod. Phys.* **57** (1985) 287.
2. B. M. McCoy and T. T. Wu, *Phys. Rev.* **176** (1968) 631.
3. D. S. Fisher, *Phys. Rev. A* **30** (1984) 960.
4. A. Altland, B. D. Simons, *J. Phys. A* **32** (1999) L353-L359.
5. P. W. Brouwer, C. Mudry, B. D. Simons, A. Altland, *Phys. Rev. Lett.* **81** (1998) 862.
6. C. Mudry, P. W. Brouwer, A. Furusaki, *Phys. Rev. B* **59** (1999) 13221; cond-mat/0004042.
7. P. W. Brouwer, C. Mudry, A. Furusaki, *Nucl. Phys. B* **565** [FS], 653 (2000).
8. P. W. Brouwer, C. Mudry, A. Furusaki, *Phys. Rev. Lett.* **84**, 2913 (2000).
9. N. Nagaosa and P. A. Lee, *Phys. Rev. Lett.* **64** (1990) 2450, V. Kalmeyer and S. C. Zhang, *Phys. Rev. B* **46** (1992) 9889; B. I. Halperin, P. A. Lee, and N. Read, *Phys. Rev. B* **47** (1993) 7312.
10. A. Furusaki, *Phys. Rev. Lett.* **82** (1999) 604.
11. T. Nagao and K. Slevin, *J. Math. Phys.* **34** (1993) 2075; J. J. M. Verbaarschot and I. Zahed, *Phys. Rev. Lett.* **70**, (1993) 3852; S. Hikami and A. Zee, *Nucl. Phys. B* **408** (1993) 415; A. V. Andreev, B. D. Simons, and N. Taniguchi, *Nucl. Phys. B* **432** (1994) 487.
12. F. J. Dyson, *Phys. Rev.* **92** (1953) 1331.
13. For a review, see C. W. J. Beenakker, *Rev. Mod. Phys.* **69** (1997) 731.
14. H. Schmidt, *Phys. Rev.* **105** (1957) 425; M. Büttiker, *J. Phys.: Condens. Matter* **5** (1993) 9361.
15. O. N. Dorokhov, *Pis'ma Zh. Eksp. Teor. Fiz.* **36** (1982) 259 [*JETP Lett.* **36** (1982) 318]; P. A. Mello, P. Pereyra, and N. Kumar, *Ann. Phys. (N.Y.)* **181** (1988) 290.

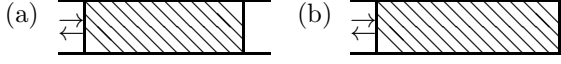


FIG. 1. Boundary conditions used for the computation of the conductance (a) and DoS (b).

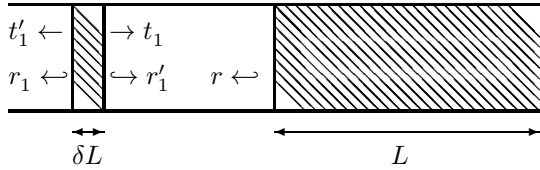


FIG. 2. A thin disordered slice of length δL is added to the left of a disordered wire of length L .

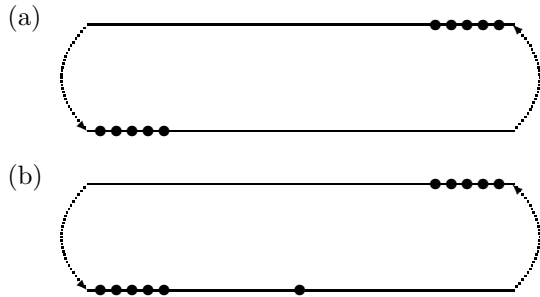


FIG. 3. The L -dependence of the eigenphases of r is described in terms of a Brownian motion of fictitious particles with coordinate u_j where $\text{Im } u = 0$ or π . If N is even, a repulsive interaction (see text) traps all particles near $u = -\ln \varepsilon \xi$ or $\ln \varepsilon \xi + i\pi$ and prohibits them from moving around (a). If N is odd, one particle can diffuse freely around the branches, and thus leads to a significantly higher DoS than for even N (b).

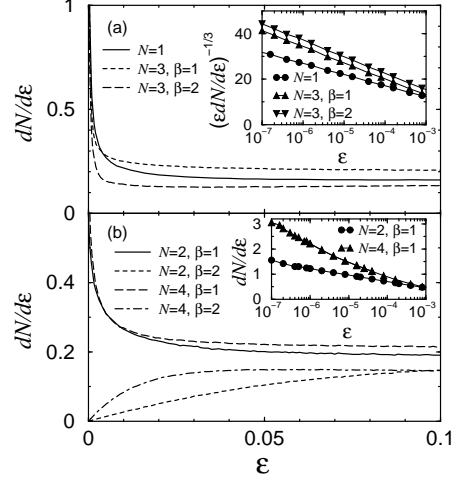


FIG. 4. Density of states, from numerical simulations for $N = 1, 3$ (a) and for $N = 2, 4$ (b). The data shown on the linear scale are computed for $L = 200$ ($L = 500$ for $N = 1$) while the data in the insets are for $L = 10^5$ ($L = 10^6$ for $N = 1$). For $\beta = 1$ and also for $N = 1$ the hopping amplitudes are taken from a uniform distribution in the interval $[0.5, 1.5]$, while for $\beta = 2$ the random flux model [6] is used, where the randomness is introduced only via the random phases of the hopping amplitudes. Results of an average over 4×10^4 – 10^6 disorder realizations are shown.

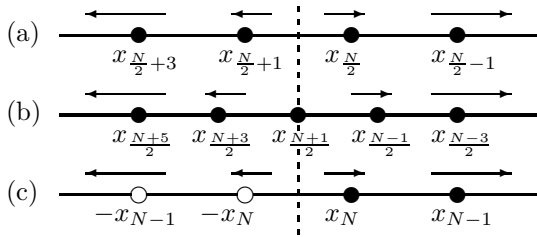


FIG. 5. For a wire with off-diagonal disorder, the L -dependence of the eigenvalues $\tanh^2 x_j$ of $r^\dagger r$ is described in terms of a Brownian motion of fictitious particles with coordinate x_j on the real axis. If N is even, all x_j (full circles) repel away from 0 (a), while $x_{(N+1)/2}$ remains close to 0 for odd N (b). In the case of diagonal disorder, all x_j repel from 0 due to repulsion from mirror images (open circles) (c).

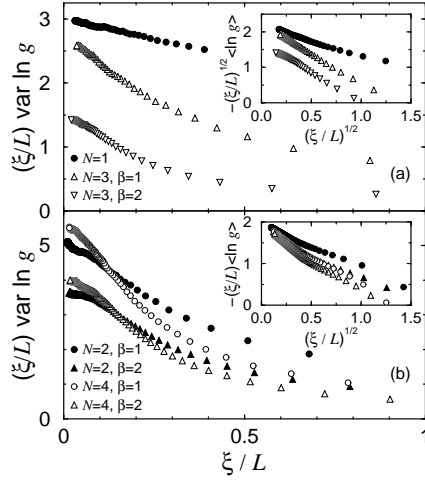


FIG. 6. Average and variance of $\ln g$ versus L/ξ for $N = 1, 3$ (a) and $N = 2, 4$ (b). The hopping amplitude t_{\parallel} is taken from a uniform distribution in the interval $[0.9, 1.1]$, while t_{\perp} is a real random numbers in $[-0.2, 0.2]$ for $\beta = 1$ and a complex random numbers with modulus < 0.1 for $\beta = 2$. The characteristic length ξ is obtained from a comparison with Eqs. (4) and (5). Results of an average over more than 2×10^4 disorder realizations are shown.